A Light Curve Simulation of The Apollo Lunar Ascent Module

Siwei Fan*, and Carolin Frueh†
Purdue University, West Lafayette, Indiana, 47907, USA
Alberto Buzzoni‡
Istituto Nazionale di Astrofisica, Bologna, 40127, Italy

According two observations that were made in 2013, an yet unknown object (later designated as WT1190F) was believed to impact Earth 2 years later in the morning of November 11th 2016 at a speed of 11 km/s. During the event, astrometric signature of the object was obtained from Loiano, Italy and DEIMOS, Spain. As a primary candidate, generating the light curve of the the long last Apollo 10 Lunar ascent module (call sign Snoopy) is useful in terms of examining the confidence level of the candidate. This paper proposes a combined approach of light curve simulation, which includes the model construction using Solidworks, further characterization of model using MeshLab, and ray tracing code to generate final results. Although the observed photometric data for object in near space is usually limited to fewer data points depending on the specific setup and observation condition, the simulation procedure proposed in this article does not suffer from these uncertainties.

Nomenclature

L	Photometric magnitude
t	Time
I_0	Solar intensity
A	Area
r	Distance, kg
C_d	Lambertian reflection coefficient
C_s	Specular reflection coefficient
$\hat{O}$	Object to observer vector
$\hat{N}$	Facet normal vector
$\hat{S}$	Object to Sun vector
τ	Specular condition check
a_{Sun}	Distance to Sun
r_{Sun}	Solar radius
η	Filter attenuation ratio
P	Assumed point of intersection
O	Light ray origin
λ	Light ray direction coefficient
$\vec{v}$	Light ray direction
b	Barycentric coordinate coefficient
Subscript	
i	Facet Count
topo	Topocentric

*PhD Student, School of Aeronautics and Astronautics
†Assistant Professor, School of Aeronautics and Astronautics
‡Senior Associate Astronomer

I. Introduction

During November 7 to November 10 2015, an yet unknown object has been observed, named WT1190F and decaying on the Earth few days after. It was in a highly eccentric orbit with a period of about 500 hours and have been spotted occasionally since 2009. Astronomers around the globe have been observing this object. Besides astrometric observations, characterization observations have been acquired. Dr.Buzzoni from INAF (Italy) was able to observe WT1190F continuously with photometric purpose on these nights including the re-entry event. Their have on average 15 observations per night during November 7 to 10. The data is rather consistent that Johnson-Cousins R_c has the most significant magnitude comparing to Johnson V and B bands, which is around relative magnitude of 20 and much more continuous observations were made during the re-entry where the average magnitude is about 15.

All these observations, light curves in general, describes the photometric intensity of certain object as time proceeds. They hence depend on the object geometry, reflection properties and the observation geometry. Characterization of light curves has a long history.Frueh came up with a probabilistic procedure to detect self-shadowing and consequently generating light curves for high area-mass-ratio objects.[5] Kaasalainen[12] are able to utilize light curves and reconstruct the geometric shape of which the light curves are based of from, which the process is called light curve inversion. Wetterer[3] was able to estimate attitude information using unscented Kalman filter whereas Cowan[4] took light curves of starts and estimated its inclination.

Among experts the hypothesis spread that the unknown object of date could be the ascent module of the Apollo 10 lunar lander. The ascent module of the Apollo lunar lander carried an important task during the moon mission. It was responsible of ferrying astronauts to and from the Lunar surface, and as a drill run to the famous Apollo 11 mission, the unmanned Apollo 10 ascent module (Snoopy) was jettisoned into Heliocentric orbit according to the mission report and went missing.

This initial hypothesis was based on the astrometric positions and recovered orbit derivations, however, those calculations have large uncertainties and cannot confirm or deny reliably if the unknown object WT1190F is in fact the Apollo module.

The characterization measurements could provide extra information in providing evidence supporting or denying the hypothesis. In this paper, the algorithm is introduced and discussed first, then example computations on trivial setups are shown to verify the algorithm, and lastly simulation results for Apollo 10 Snoopy at multiple attitude states is presented.

II. Simulation Scheme

Fig. 1 shows the operation scheme for the simulation. A combined simulation approach is to be followed here that simpler geometries can be defined directly in the simulation environment, whereas the use of polygon file (.ply) enables us to import more complex object shapes (e.g. a satellite or pieces of satellite). Ray tracing code will take the object information as well as other orbital information as input to generate light curves.

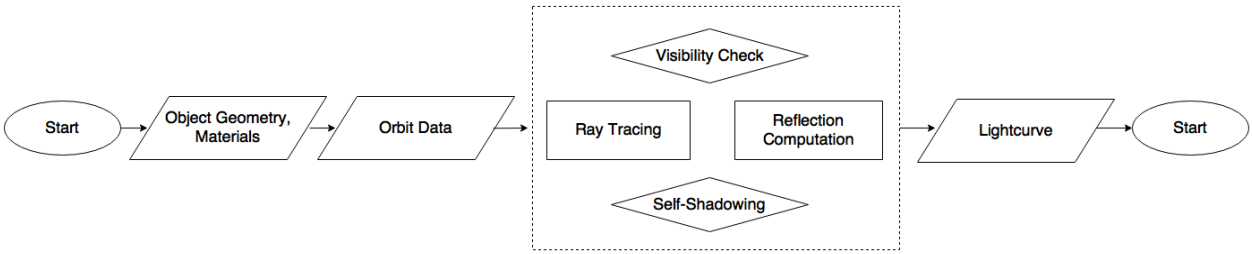

Figure 1: Simulation Flowchart

A. Orbit

The orbit data for WT1190F as well as the Sun is extracted from JPL's HORIZONS system, originally in range, right ascension and declination. Loiano Observatory in Italy is picked as the observer location. All position is then converted from J2000 to true of date. The period of time is picked to start with 1 minute

interval from 0 UTC on 6-Nov-2016 to 6 UTC on 13-Nov-2016, where reentry event of WT1190F happens half hour after. **Fig.2a** shows the object orbit during this period, where the range covers from 11656.7 km to 583276.8 km. The rapid decrease in phase angle (**fig.2b**) is due to the rapid approaching towards the observer. The fact that Earth is to scale in the orbit plot also justifies this sudden decrease. Due to the scale, only the direction towards Sun is shown. There are 10441 data points for position vector and time vector.

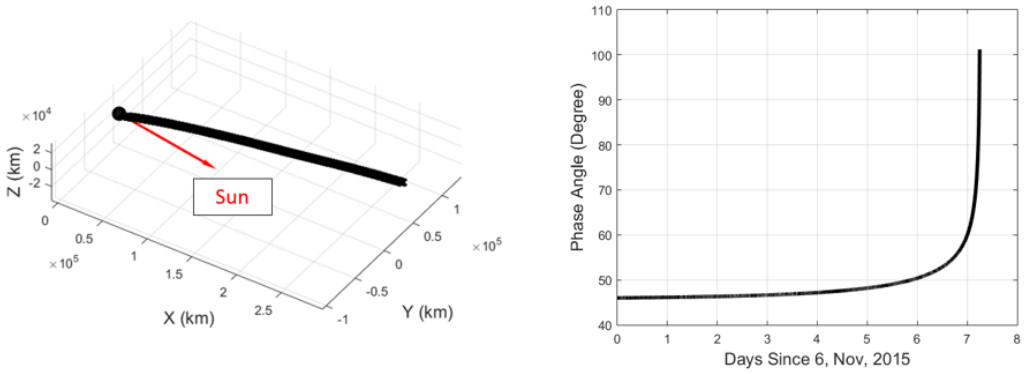

Figure 2: WT1190F Orbit and Phase Angle Plot

B. Object Model

Objects with arbitrary complexity can all be simulated given their polygon file. Such file format is commonly used in the area of computer graphics. A typical polygon file is consist of 3 lists, 1) coordinates of all vertices, 2) face list defined by its vertices (triangular mesh in this case), and 3) color of each face to define its optical property. These are precisely the 3 things we need to perform light reflection calculation.

Fig.2a is the original modeling used for Snoopy, it includes many small features like the attitude control nozzles, hand rails, docking lights, windows and various antennas. Some of these curved details require a lot of tiny meshes but do not result significant difference in relative magnitude.

Fig.2b shows the model excluding these small features.More mesh is generated using a midpoint subdivision algorithm in MeshLab. This is because the lighting condition of each facet is determined only at its center in the ray tracing algorithm. Simply speaking, if a plate is given, part of it can be in the shadow while rest of the plate still reflects light. As a result, the finer the mesh, the more accurate the result, which leads to **fig.2c**

Fig.2d adds material on top of **fig.2c**, aluminum (Al) and silicon carbide (SiC). This is trying to recover the surface material of Snoopy as close as possible. The use of aluminum in space is no secret although the spectral property of aluminum depends highly on its finishing. To be conservative, I assumed 0.9 as Lambertian reflection coefficient and almost 0.1 for specular reflection coefficient. The other material is SiC. It is an antioxidation paint that can withstand extreme thermal cycling (up to 1400^oC), which agree with space application. Its most noticed optical property is the high solar absorption of 0.9.[6] This coefficients are related to the reflection model chosen which is talked about in the next section.

C. Ray Tracing Computation

In the ray tracing code, several checks are implemented to determine whether a facet is visible to the observer: 1) the facet has to be above observer's local horizon; 2) the observer and the Sun has to be above facet's local horizon at the same time or else either the facet cannot be seen or it is never being shined on; 3) parts of the object does not obstruct the light rays coming in and going out on the facet (i.e. self-shadowing check). Only when a facet passes these checks, will the algorithm continue to compute the light intensity (0 intensity if check fails).

Usually, if you want to simulate the light curve during the period when actual observation was made, condition 1 is met because you would get no observation otherwise. Condition 2 will rule out lots of facets

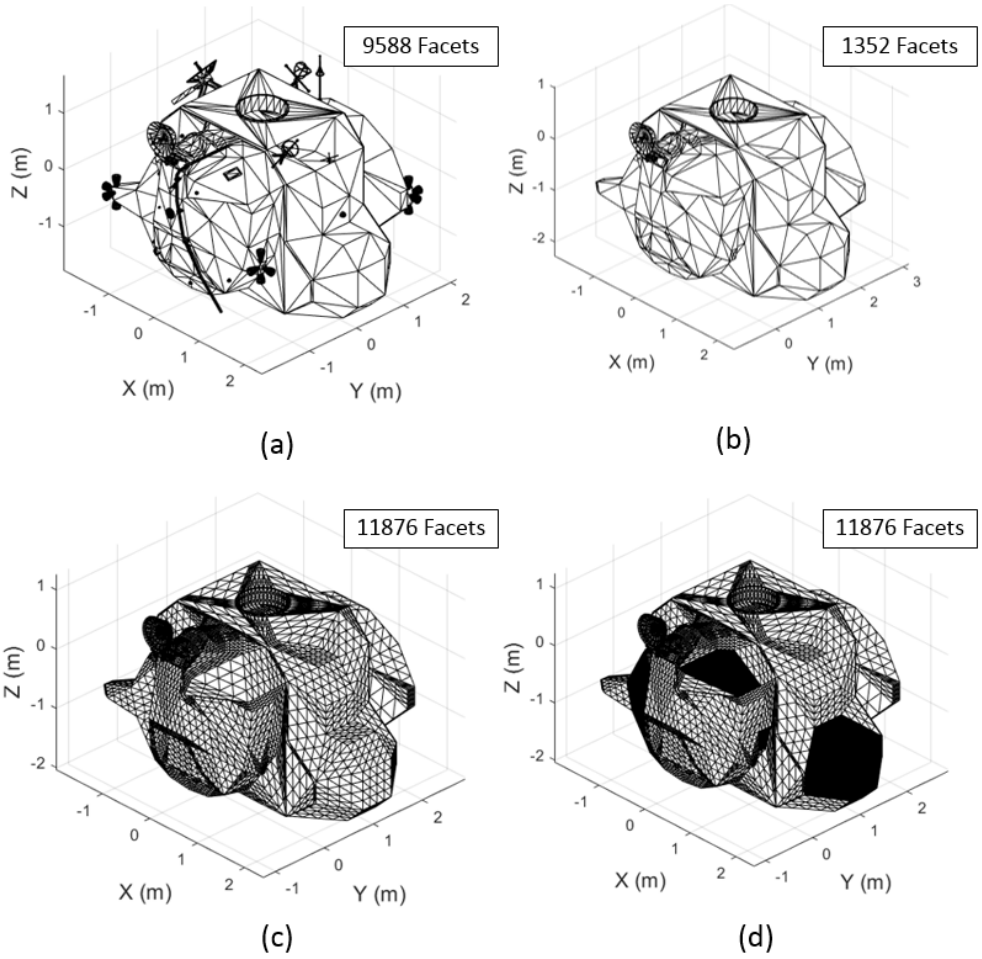

Figure 3: Mesh Demonstration

and speed up the computation at least 2x, because one can only observe half the sphere at best regardless (at small phase angle).

Condition 3 takes the longest to check because theoretically one has to go through all other facets to check the self-shadowing on one facet and this has to be done twice for light source and observer. Commercial rendering tools are often able to reduce runtime here through narrowing check to vicinity or local for example. 100% accurate computation for every single facet is usually not their goal. For this step, the Moller-Trumbore intersection algorithm is implemented. Its purpose is to determine whether there is an intersection between a ray originated from point **O** and the triangle given its vertices P_1, P_2, and P_3 as seen from **fig.4**.

Eq.1 is the representation of a ray, **eq.2** represents all the points within the triangle given b_1 and b_2. If such point **P** exists, then the light ray does get obstructed.

$$P = O + \lambda\vec{v} \quad \text{where} \quad (0 \geq \lambda) \tag{1}$$

$$P = P_1 + b_1(P_2 - P_1) + b_2(P_3 - P_1) \quad \text{where} \quad (0 \leq b_1 \leq 1, 0 \leq b_2 \leq 1, b_1 + b_2 \leq 1) \tag{2}$$

Equating **eq.1** and **eq.2**,

$$O + \lambda\vec{v} = P_1 + b_1(P_2 - P_1) + b_2(P_3 - P_1) \tag{3}$$

$$O + \lambda\vec{v} = P_1 + b_1\vec{e}_1 + b_2\vec{e}_2 \tag{4}$$

$$\begin{bmatrix} -\vec{v} & \vec{e}_1 & \vec{e}_2 \end{bmatrix} \begin{bmatrix} \lambda \\ b_1 \\ b_2 \end{bmatrix} = O - P_1 \tag{5}$$

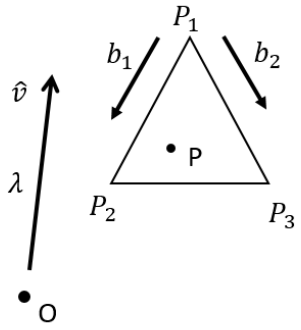

Figure 4: Moller-Trumbore Intersection

It can be seen that this method of detecting self-shadowing is indeed exact, but do not forget about the problem mentioned in the previous chapter that finer mesh will produce more accurate result. For this specific Apollo model, the number of facets used (**fig.2c**) is sufficient to generate meaningful result. Objects with more severe concavity will naturally experience more self-shadowing, and increasing the number of facets may then be required. Another point worth mentioning here is that, not only do the set of equations has to yield real numbers for λ, b_1, and b_2, the value has to fall into the correct range as well. For example, if λ is found to be a negative number, this means the triangle is in the opposite of the ray direction $\vec{v}$, and no intersection will occur. If b_1 and b_2 violate the inequalities, that means the ray will hit somewhere else in the same plane as the triangle, but not inside of it.

After a facet passes all these checks, the Lambertian reflection is calculated using the basic bi-directional reflection model (BRDF) as **eq. 6** suggests. **eq.7** is the condition for specular reflection, it is allowing half a degree difference between the incoming and the outgoing light ray to compensate for the size of Sun, although in relative position computation, the Sun is still treated as a point source.

$$L(t) = I_0 \sum_{i=1}^{n} \frac{A_i}{\pi (r_{topo}(t))^2} [C_d(\hat{O}_i.\hat{N}_i)(\hat{S}_i.\hat{N}_i) + \frac{\tau_i C_s (r_{Sun}(t))^2}{a_{Sun}^2}] \tag{6}$$

$$\tau_i = \begin{cases} 1, if|\theta_{incoming} - \theta_{outcoming}| \leq 0.5^o \\ 0, else \end{cases} \tag{7}$$

I_0 refers to the irradiance of the sun at 1 AU which is about $1365 W/m^2$. Specular condition check τ equals to 1 or 0 depending on whether specular reflection is met (**eq. 7**), half a degree is allowed here because we do not consider Sun as a point source. Additionally no limb darkening effect is taken into account. Overall, if there is self-shadowing, the intensity contribution from that facet would be 0. Several examples will be presented later to provide validity of this reflection model.

Conventionally, light curve uses another unit called relative magnitude (because it is comparing with a constant value of solar magnitude) which can be calculated from irradiance using **eq. 8**. The more negative the magnitude gets, the brighter the object, and as a reference, the magnitude limit for naked human eye is about 6. There are also different conventions and sources for the magnitude of the Sun, we use -26.74 in our simulation.

$$mag_{sphere} = mag_{Sun} - 2.5 log_{10}(\frac{L_{sphere}}{I_0}\eta) \tag{8}$$

η in **eq.8** is a ratio used to simulated the filter mounted on the telescope. It has to first assume that the Lambertian reflection model is primarily for the visible spectrum. Then, the American Society for Testing and Materials published in the year of 2005 a table to reference solar spectral irradiance value (**Citation for Air Mass 1.5?**). By using this table and the Johnson-Cousins R filter curve, a ratio of unfiltered irradiance and total irradiance can be computed. This ratio η is about 0.2834 if considering wavelength from 280 nm to 800 nm, in other words about 72% of the total intensity is lost for the waveband considered. As a result, this will cause the relative magnitude to increase by about 1 whole magnitude.

III. Simulation Result

Several test example light curve will be presented to help verify the validity of the reflection model used and the self-shadowing algorithm. Then, simulation result for Apollo 10 lunar ascent module at different attitude states will be shown to illustrate the program's capability.

A. Sphere and Plate Example

The sphere is an excellent choice to act as the first test of the program. It is perfectly concave, its attitude motion does not affect the result at all, and there are analytical solution (**eq.9**) to the light curve of a sphere with radius r.

$$mag = mag_{Sun} - 2.5log_{10}[\frac{4r^2C_d(sin\theta + (\pi - \theta)cos\theta)}{(x - r_{Earth})^2}] \tag{9}$$

θ is the phase angle of the sphere, x is the distance between object and Earth center, and notice there is only Lambertian reflection coefficient here. **Fig.5a** is a sphere generated using cube mapping technique for demonstration purpose, the actual sphere consists of more facets than shown. This mapping will allow the sphere to look almost exactly the same regardless of the viewing angle just like a perfect sphere. To demonstrate the agreement of analytical and simulation result, the specular reflection is turned off. As seen from **fig.5b**, the object is brighter at smaller phase angle and darker at larger phase angle. This agree with the situation where full moon happens when Earth is between Sun and Earth moon, whereas the observer will see less than half a sphere when the moon is in between. There still are small error as seen from **fig.5b**, this is possible due to the imperfect modeling of a perfect sphere and 0.9 as Lambertian reflection coefficient which the analytical result assumes pure Lambertian.

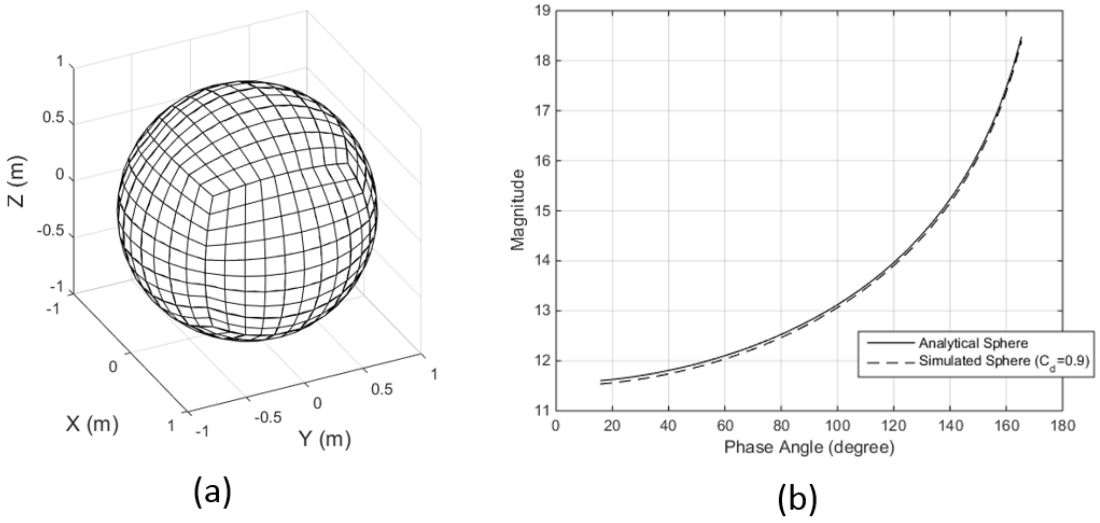

Figure 5: Sphere Lightcurve

The Iridium flare is a well known event that can be observed directly by naked eyes. It is caused by alignment of the main mission antenna (MMA) of Iridium communication satellite which is made of Aluminum with the size of about a door (**fig.6a**). For this setup, I fixed Sun at 1 AU in positive x-axis, and observer starting position at 1 Earth radius in positive x-axis. Then created an orbit at 666 km such that it will produce a glint. **Fig.6b** shows the light curve of this setup, it was let to propagate for 30 minutes. 0.9 was used as specular reflection coefficient, which makes it behave similar to a mirror. This is a reasonable value considering the actual magnitude of an iridium flare is about -8 to -4 range depending on situations.

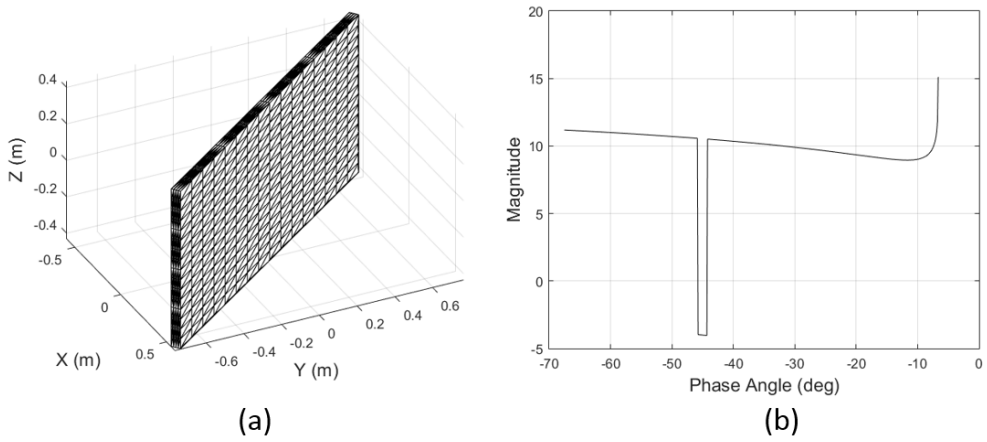

Figure 6: Iridium Flare Lightcurve

B. Apollo 10 Lunar Ascent Module Simulation

For this section, Apollo 10 LEM was put on the orbit and first scenario where the object is fixed to orbit orientation is simulated first. **Fig.7** shows the result comparison when self-shadowing and specular reflection is turned off. A general trend of gradually decreasing in magnitude can be observed. Notice with just 10% specular reflection component, several lucky spikes due to specular reflection which causes major bright magnitude can be seen. The difference in magnitude when self-shadowing is turned off is about 8 magnitude. Given that the unit is in log scale, this means that the difference in result is very significant and self-shadowing can not be ignored since it will come back to the same position under lower RPM.

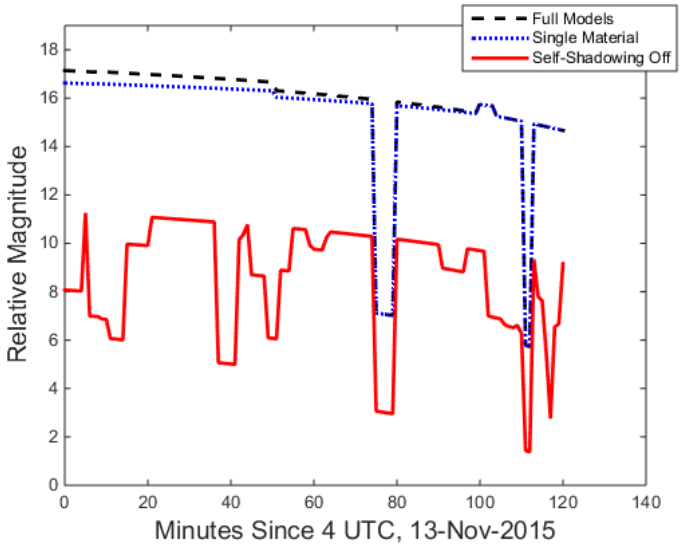

Figure 7: Lightcurve Comparison for Space-fixed Orientation of the Object

The second scenario is that the object is spinning about its maximum or minimum principle axis. From an observed light curve, methods exist to extract pole and spin axis for less complicated shapes in solar system[78] . However, our object has significant convexities. Its principle axis is calculated assuming the whole module to be a thin aluminum shell of 0.5 *cm*. With the starting orientation of the object and the axis of rotation are known, all that left is the spin rate. The exact spin rate extraction is subject to another research thrust and not detailed here. Instead a few common sense rules are followed here, if the time

resolution of orbit data is exactly one minute, to illustrate the rotating object cases and its effects on the light curve: 1) avoid integer or close to integer angular velocity so it does not always end up in the same orientation it started with, 2) choose less than 1 RPM to give you more insight on the progressive effect of self spinning, result from higher-than-1 RPM is just going to repeat.

From **fig.8**, the result is showing gradual increasing brightness due to Earth-approaching orbit, and notice that the oscillation in light curve is similar for spinning around both axis. Additionally, the vehicle does not complete even a single full revolution during the 2 hour time.

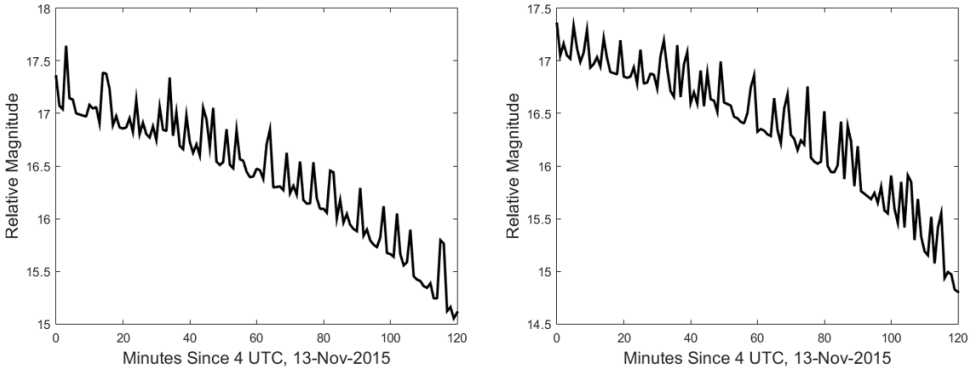

Figure 8: Lightcurve for 0.008 RPM about Minimum and Maximum Inertia Axis with Self-Shadowing

Fig.9 shows the result for a much higher RPM of 0.15. It is surprisingly smooth, lack of short period oscillation. Both results again behave similarly and this just shows a different taste of result when different combinations of object attitude and location come together.

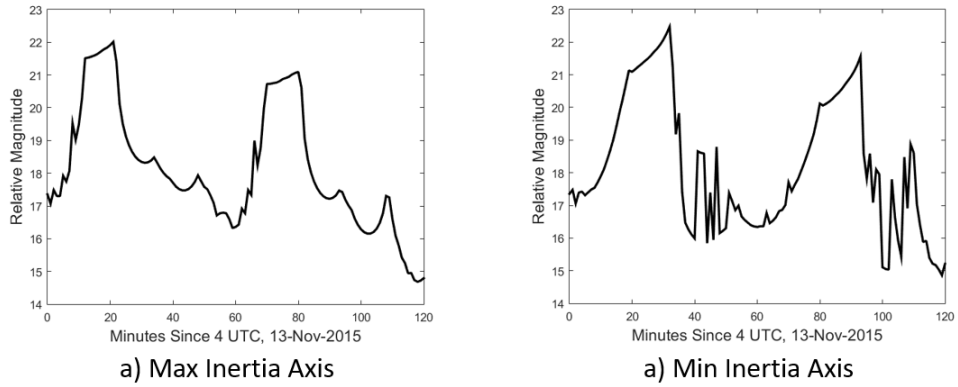

Figure 9: Lightcurve for 0.15 RPM about Minimum and Maximum Inertia Axis with Self-Shadowing

There are also less common cases that spinning about these two axes would result in the opposite trend. However, this study does not focus on trying to come up with a global minimum solution that replicate observation data. Because the simulation result is rather sensitive to the object attitude input, and with the presence of observation uncertainty, it is only possible to deduce the conclusion that whether or not the object is remotely close to the Apollo 10 LEM.

This can be done through the third scenario. It involves finding the orientations of Apollo 10 LEM that will cause maximum and minimum brightness and try to bound the observation data. **Fig.10** for example gives these orientations on 4 UTC, 13-Nov-2015. Same technique can also be extended to find orientations for other time instance.

Fig.11 shows the summary of the result where all data point (dots) lie well within the boundary. Considering it is in log scale, a magnitude of 25 and above is already very faint, thus the upper bound (lower brightness) are roughly on the same level. The lower bound (higher brightness) are all caused by specular

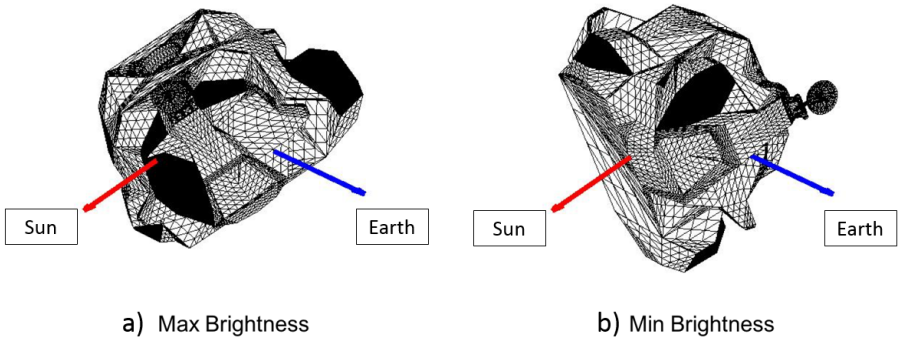

Figure 10: Best and Worst Orientation for A Time Instant

reflection. Most results/orientations lie within a narrower region (roughly 13 to 22). Overall, this concludes that Apollo 10 LEM is indeed a possible candidate to the unidentified WT1190F.

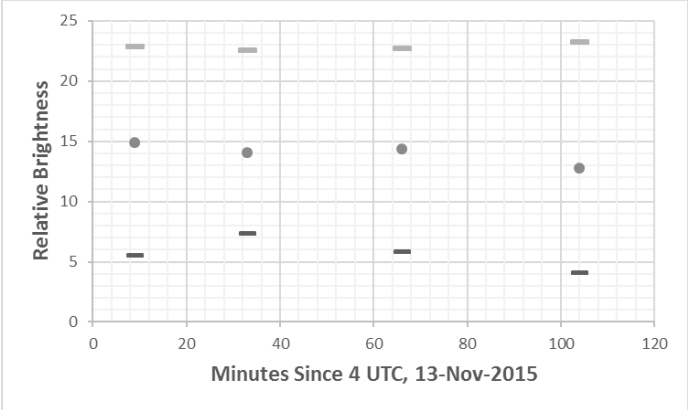

Figure 11: Darkest and Brightest Orientations Bound the Data Point

IV. Conclusions

The light curve simulation provides a general approach to generate light curve. By introducing the polygon file, generating light curves for virtually any object is possible. The simulation includes two reflection models which are validated by either analytical result or real observation. The self-shadowing detection is the important piece to bring nonlinearity into the simulation environment and the result is believed to be closer to reality.

Specific conclusions about simulation results are: Self-shadowing causes significant difference in relative magnitude; the darkening peak feature is present for all simulation runs; orientations can make very significant difference in terms of the relative magnitude; and Apollo 10 LEM is a possible candidate to the puzzling case of WT1190F.

The ability to simulate light curve is a necessary part of the bigger picture, where more accurate result can only be more beneficial to the study of identifying space objects.

References

[1]Kaasalainen, M., Lamberg, L., Lumme, K., and Bowell, E., 1992 *Interpretation of light curves of atmosphereless bodies, I. General theory and new inversion schemes.* Astron. Astrophys. 259, 318-332.

[2]Kaasalainen, M., and Torppa, J., 2001 *Optimization Methods for Asteroid Lightcurve Inversion. I Shape Determination,*

Icarus, 153, 24-36.

[3]Wetterer, C. J., Jah, M., (2009), Attitude Estimation from Light Curves. *Journal of Guidance,Control, and Dynamics, Vol.32, No.5, Sept-Oct 2009.*

[4]*Cowan, N., Fuentes, P., Haggard, H., (2013). Light curves of stars and exoplanets: estimating inclination, obliquity and albedo. Mothly Notices of the Royal Astronomical Society, 434,p.2465-2497.*

[5]*Frueh, C., Kelecy, T., Jah, M., Coupled Orbit-Attitude Dynamics of High Area-to-Mass Ratio (HAMR) Objects: Influence of Solar Radiation Pressure, Earth's Shadow and the Visibility in Light Curves, itCelestial Mechanics and Dynamical Astronomy, 117:385404, 2013.*

[6]*Scheffler, M., and Colombo, P., (2006). Cellular Ceramics: Structure, Manufacturing, Properties and Applications. John Wiley & Sons, Ltd, 526. doi:10.1002/3527606696.ch5g*

[7]*Kaasalainen, M., (2001).Interpretation of lightcurves of precessing asteroids, Astronomy and Astrophysics. 376, 302-309*

[8]*Lumme, K., Karttunen, H., and Howell, E., (1990). A Spherical Harmonics Method for Asteroid Pole Determination, Astronomy and Astrophysics. 229, 228-239*